Cerebral Cortex March 2007;17:591-598
doi:10.1093/cercor/bhk004
Advance Access publication April 20, 2006

White Matter Pathway Asymmetry Underlies Functional Lateralization

Thomas R. Barrick[1], I. Nigel Lawes[2], Clare E. Mackay[3] and Chris A. Clark[1]

[1]Centre for Clinical Neuroscience, Division of Cardiac and Vascular Sciences and [2]Department of Basic Medical Sciences, St George's University of London, Cranmer Terrace, London SW17 0RE, UK and [3]University Department of Psychiatry and Prince of Wales International Centre, Warneford Hospital, Headington, Oxford OX3 7JX, UK

Structural and functional asymmetry of the human brain has been well documented using techniques such as magnetic resonance imaging (MRI). However, asymmetry of underlying white matter connections is less well understood. We applied an MRI technique known as diffusion tensor tractography to reveal the morphology of the white matter in vivo by mapping directions of maximum water diffusion in brain tissue. White matter pathway asymmetry was investigated in a normalized image data set of 30 right-handed young healthy individuals. We identified, for the first time, a rightwardly asymmetric pathway connecting the posterior temporal lobe to the superior parietal lobule. This pathway may be related to auditory spatial attention and working memory for which there is evidence for a rightward laterality from functional imaging studies. Additional leftward asymmetries connecting the parietal and frontal lobes to the temporal lobe may be more closely related to laterality of language.

Keywords: asymmetry, brain, diffusion tensor tractography, functional lateralization, MRI

Introduction

Asymmetrical structure–function relationships have been studied in the human brain since Broca (1861) identified a major functional asymmetry, whereby speech production is linked preferentially to the left hemisphere for the majority of people. Since Broca (1861), lesion studies and, more recently, functional neuroimaging studies have established hemispheric specificity for a range of language, motor, and spatial tasks (Davidson and Hugdahl 1995), but their relationship to underlying gray and white matter anatomy remains unclear. A frequently cited structure–function relationship in the human brain is between leftward (i.e., left greater than right) planum temporale asymmetry and hemispheric dominance for language function (Geschwind and Levitsky 1968). The planum temporale is a large region of auditory association cortex located on the superior temporal plane posterior to Heschl's gyrus involved in verbal and nonverbal stimuli (Griffiths and Warren 2002). It has been reported to have leftward asymmetry in postmortem (Geschwind and Levitsky 1991), magnetic resonance imaging (MRI) volumetry (for review, see Shapleske and others 1999), and voxel-based MRI asymmetry studies (Good and others 2001; Watkins and others 2001; Barrick and others 2005). This structure–function relationship is further supported by reports of reduced morphological asymmetry in patients with language disorders such as dyslexia (e.g., Rumsey and others 1986).

Recently, the temporal lobes have been implicated in auditory dual-pathway (what and where) networks that involve the frontal and parietal lobes (Rauscheker 1998; Romanski and others 1999; Clarke and others 2000, 2003; Zatorre and others 2002; Arnott and others 2004; Hickok and Poeppel 2004). In addition to language laterality, lateralized function of auditory spatial processing and attention in the inferior parietal lobule are reported in functional imaging studies (Griffiths and others 1998; Weeks and others 1999; Zatorre and others 1999, 2002; Griffiths and others 2000; Itoh and others 2000; Alain and others 2001; Brunetti and others 2005). Furthermore, functional laterality in the superior parietal lobule is also reported (Griffiths and others 1998, 2000; Zatorre and others 1999; Macaluso and others 2004).

This extensive literature describing asymmetry of brain morphology and function implicates the temporal, frontal, and parietal lobes. However, the anatomy of white matter pathways related to these asymmetries remains to be determined. In particular, investigations that provide greater anatomical specificity of the underlying white matter will contribute to an understanding of cerebral asymmetry at the cortical and functional level. In the present study, we examine the cerebral asymmetry of white matter architecture imaged by mapping water diffusion characteristics from diffusion-weighted MRI. This technique, known as diffusion tensor tractography, is the only noninvasive method currently available for investigation of white matter organization and hence, the underlying connectivity of the brain. Although connectivity of individual axons cannot be inferred, tractography provides information on the order of magnitude of a millimeter and has been applied to reconstruct anatomically plausible commissural (Catani and others 2002; Mori and others 2002; Hagmann and others 2003), association (Catani and others 2002; Mori and others 2002; Hagmann and others 2003), and projection fibers (Behrens and others 2003; Johansen-Berg and others 2005) as well as white matter in the midbrain (Stieltjes and others 2001), fornix (Catani and others 2002; Hagmann and others 2003), and cingulum (Catani and others 2002; Hagmann and others 2003).

Diffusion tensor tractography has recently been applied to describe left hemisphere language-related white matter pathways (Catani and others 2005). Moreover, Parker and others (2005) reported that 2 of the 3 language pathways described by Catani and others (2005) are leftwardly asymmetric. Catani and others (2005) and Parker and others (2005) reconstructed white matter structure by extracting pathways passing through, or originating from, user-defined regions of interest. Because the gross gray and white matter anatomy of the temporal lobe is asymmetric (Barrick and others 2004, 2005), manually defining regions of interest can lead to anatomical bias and potentially erroneous assignment of asymmetry to white matter pathways. In the present study, we remove any bias that may occur from application of user-defined regions of interest by reconstructing white matter pathways that pass between entire cerebral lobes

segmented in standardized space (Evans and others 1993) using a map of segmented cerebral structures known as the Talairach Daemon (Lancaster and others 2000). We apply this fully automated lobe-based tractography technique to investigate the underlying morphology and asymmetry of all white matter pathways that connect the temporal lobe to the parietal and frontal lobes of 30 young healthy right-handed subjects. Novel visualization techniques are introduced to define the anatomy of white matter pathway asymmetry in terms of symmetrical streamline color (SSC) and intersubject variability maps. For the first time, we reveal a significant asymmetry of white matter pathways, connecting the superior and middle temporal gyri to the superior parietal lobule that may be related to laterality of auditory spatial function and auditory working memory. Significant white matter pathway asymmetries associated with language function are also found, in agreement with previous studies.

Materials and Methods

Data Acquisition

Diffusion-weighted images were acquired for 30 right-handed healthy volunteers (15 males, 15 females, ages 20–39 years, mean age 27.2 ± 5.2 years) from whom informed written consent had been obtained to participate in the study. Diffusion-weighted images were obtained using a diffusion-sensitized spin echo–planar imaging sequence using a 1.5-T General Electric Signa MRI system equipped with magnetic field gradients of up to 22 mTm^{-1} (GE Electric, Milwaukee, WI) and a proprietary head coil (50 × 2.8–mm thick interleaved slices, field of view 240 × 240 mm^2, matrix 96 × 96 were reconstructed on a 256 × 256–matrix giving a final resolution of 0.9375 × 0.9375 × 2.8 mm^3). Following an acquisition without diffusion sensitization (b = 0), images were acquired with diffusion gradients applied (b = 1000 s mm^{-2}) in 12 directions to eliminate diffusion-imaging gradient cross terms (Barrick and Clark 2004). The acquisitions were repeated 4 times in order to improve signal to noise ratio.

Image Analysis

Data were analyzed on an independent workstation (Sun Blade 1500; Sun Microsystems, Mountain View, CA). Images were realigned to remove eddy current distortions (Woods and others 1993). Diffusion tensor elements were computed at each voxel as described by Basser and others (1994) and diagonalized to determine the eigenvalues and eigenvectors. Normalization of diffusion tensor imaging to the standardized space of Evans and others (1993) was achieved using previously reported methods (Barrick and Clark 2004). All normalized DTIs were skull stripped using brain extraction tool (Smith 2002), part of the Oxford Centre for Functional Magnetic Resonance Imaging of the Brain software library (FSL) (Oxford University, Oxford, UK, http://www.fmrib.ox.ac.uk/). From the 30 normalized skull-stripped DTI images, a group-averaged mean DTI was computed (Jones and others 2002). For each normalized DTI and the mean DTI, fractional anisotropy (FA) maps were computed (Pierpaoli and Basser 1996).

Diffusion Tensor Tractography

Tractography was performed to determine the white matter pathways that pass from the temporal lobe to the frontal and parietal lobes in the left and right cerebral hemispheres. Streamline tractography was seeded from the center of every voxel throughout the entire brain of the 30 normalized DTIs and the mean DTI by application of a previously reported tractography algorithm (Barrick and Clark 2004). Streamline tracts were initiated in orthograde and retrograde directions from each image voxel and were iteratively followed by moving 1 mm in the direction of the principal eigenvector. Tracts were terminated in regions of low FA to allow tracts to pass into gray matter (FA $\geq$ 0.08). No angular threshold was applied on coincident principal eigenvector orientations.

Lobe Segmentation

Termination points for each individual tract (x, y, z coordinates in millimeters within standard space) were determined, and temporoparietal and temporofrontal tracts were retained in the left and right hemispheres if their terminations lay within the temporal lobe and either the parietal or the frontal lobes. Segmentations of the left and right temporal, frontal, and parietal lobes in standard space were obtained using an image found within mri3dX (http://www.aston.ac.uk/lhs/staff/singhkd/mri3dX/mri3dX.jsp), which utilizes a stored representation of the Talairach Daemon Database (Lancaster and others 2000). Using this functionality, any brain voxel can be labeled with one or more of the 5 levels within the database (i.e., hemisphere, lobe [which also includes the limbic system and deep white matter], neuroanatomical structure, tissue type, and Brodmann area [BA]). To allow for differences in morphology between single subjects and the Talairach Daemon, the termination coordinates were labeled by hemisphere and lobe by determining the shortest 3-dimensional Euclidean distance to the Talairach Daemon labels in standard space.

Computation of White Matter Pathway Intersubject Variability and Asymmetry Maps

Maps representing the pathway intersubject variability and asymmetry of temporofrontal and temporoparietal white matter pathways in the 30 normalized DTIs were computed. For each subject, voxelwise binary images containing 0 or 1 at each voxel were generated for the temporofrontal and temporoparietal tracts in the left and right hemispheres by determining whether tracts passed through image voxels (0 = outside pathway, 1 = inside pathway). A map representing intersubject variability in pathway morphology across the 30 subjects was generated by calculating the mean of these binary images for the temporofrontal and temporoparietal pathways in the left and right cerebral hemispheres. Pathway variability maps represent the normalized frequency at which tracts pass through each image voxel in standard space (i.e., 0 = no tracts pass through the voxel in any subject, 1 = tracts pass through the voxel in every subject). Pathway asymmetry maps were generated by reflecting the pathway variability maps for the left hemisphere in the midsagittal plane of standard space (i.e., the plane x = 0 mm) and subtracting the reflected left hemisphere map from the unreflected right hemisphere map. Pathway asymmetry maps represent the difference in normalized frequency between the left and right hemispheres (i.e., –1 = tracts pass through the voxel in each subject for the left hemisphere, but none pass through the homologous right hemisphere voxel, 0 = no tracts pass through the voxel in any subject, 1 = tracts pass through the voxel in each subject for the right hemisphere, but none pass through the homologous left hemisphere voxel).

Nonparametric Statistical Analysis of Pathway Asymmetry

Parametric statistical tests are unsuitable for the analysis of the voxelwise binary images representing temporoparietal and temporofrontal pathways because the assumption of a normal distribution of data at each image voxel across the 30 subjects is violated. Consequently, a nonparametric statistical test was applied to investigate the anatomy of cerebral white matter pathway asymmetry. McNemar's test (Siegel 1956) was applied on a voxel-by-voxel basis to investigate the null hypothesis of no significant difference between the numbers of subjects with leftward or rightward asymmetry. In particular, McNemar's test assesses the significance between 2 dependent samples when the variable of interest is a dichotomy. In the present study, the 2 dependent samples are homologous voxels in the left and right cerebral hemispheres, and the variable of interest is a binary number, representing whether white matter pathways are absent (=0) or present (=1) in the voxel. Temporoparietal and temporofrontal left and right hemisphere binary pathway images of the 30 subjects were statistically analyzed (N.B. all left hemisphere binary images were reflected in the plane x = 0 of standard space), and statistical results were transformed to the z statistic. Multiple comparisons correction was performed at the cluster level using FSL (Oxford University, Oxford, UK, http://www.fmrib.ox.ac.uk/). The z statistic was thresholded at $z > 2.3$, and multiple comparisons correction applied at $P < 0.001$ over the analyzed volumes.

Tract Representation for the Mean DTI

3-dimensional white matter pathway reconstructions illustrating average morphology and asymmetry were computed from the mean DTI in standard space. Individual tract termination coordinates in standard space were used to generate tract-specific RGB colors such that if symmetrical pathways are present, they are illustrated using the same color in both hemispheres, whereas if pathways are asymmetrical, they are illustrated using different colors in the left and right hemispheres. This new color scheme is referred to as the SSC map. Temporofrontal and temporoparietal tract termination x, y, and z coordinates in standard space were scaled such that all coordinates lay between 0 and 255. x termination coordinates were scaled from 0 at the left of the brain to 255 at the midsagittal plane ($x = 0$ of standard space) and back to 0 at the right. y (and z) coordinates were scaled from 0 at the posterior (inferior) of the brain to 255 at the anterior (superior) of standard space. These scaled termination coordinates were separated into start and end coordinates for each tract. Start coordinates were defined as lying more laterally than end coordinates. For each tract, the scaled start and end coordinates were divided by 16 and rounded to 4-bit binary numbers between 0000 (i.e., 0) and 1111 (i.e., 15). Eight-bit binary numbers representing the 3 components of the 24-bit RGB SSC were constructed for each of the x (red RGB component), y (green RGB component), and z (blue RGB component) termination coordinates by placing the start and end 4-bit numbers side-by-side and computing the 8-bit components of the RGB color, the merged 4-bit numbers represent. For example, if $x_{start} = 0101 = 5$ and $x_{end} = 1101 = 13$ for a single streamline, then the red component of the RGB color is 01011101 = 93. By performing this operation for each tract, the SSC was generated and applied to the white matter pathway reconstructions illustrated in the present study.

Results

Temporoparietal Pathway Morphology and Asymmetry

Two large pathways were found to pass from the posterior temporal to the parietal lobe. SSC maps indicating the average asymmetry of reconstructed temporoparietal pathways are shown in Figure 1. Because each pathway is colored according to its start and end coordinates in standard space, symmetrical pathways will have the same color, whereas asymmetrical pathways will have different colors in the left and right hemispheres. Intersubject pathway variability and asymmetry maps of the temporoparietal pathways are shown in Figure 2. Pathway variability maps use a hot color scheme (black through red to yellow) to indicate the frequency with which white matter pathways pass through each voxel in the brain. Asymmetry maps are shown to the right of pathway variability maps in Figure 2 and are colored according to the difference in pathway variability between the hemispheres. Specifically, rightward and leftward pathway asymmetries are colored by hot and cold

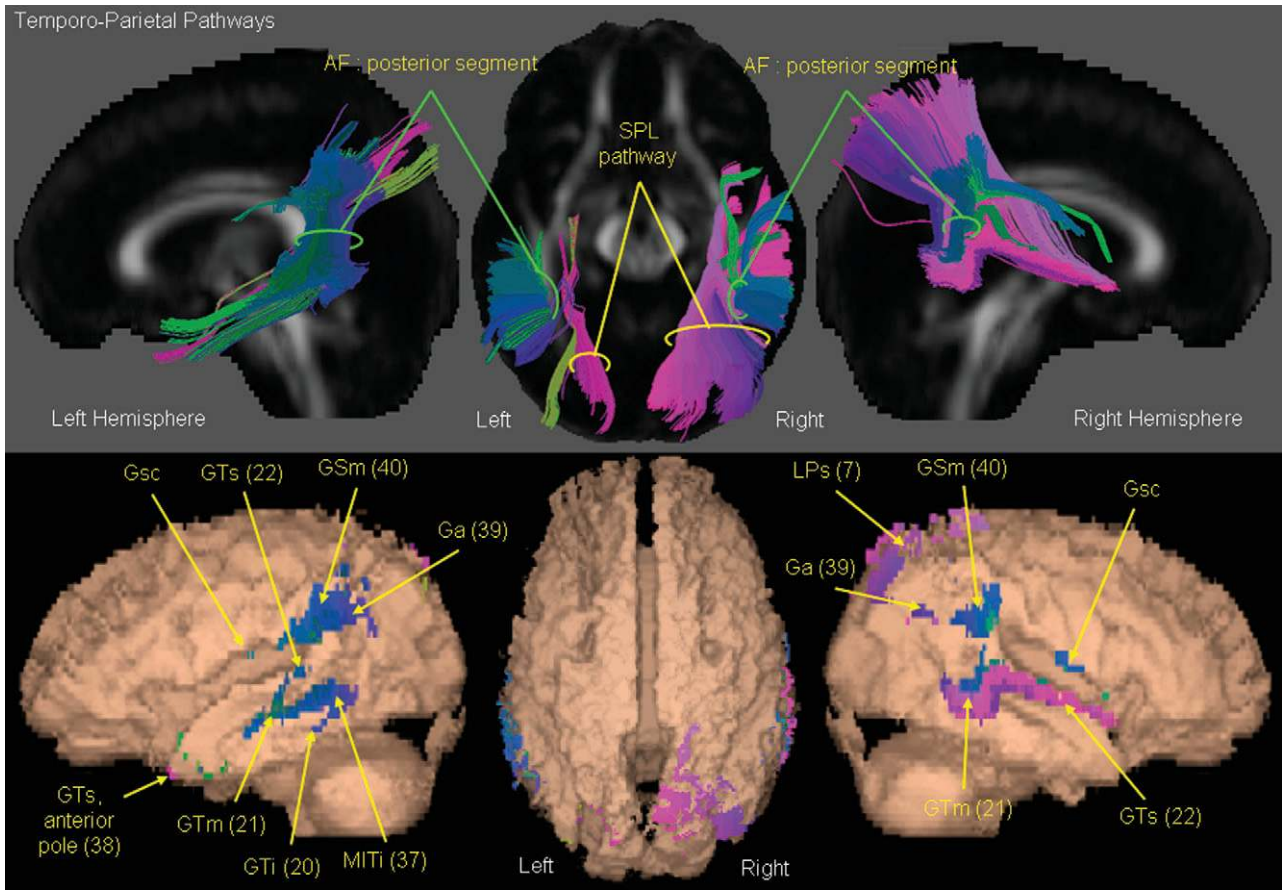

Figure 1. Temporoparietal white matter pathways. White matter fibers are illustrated that pass between the temporal and parietal lobes in the left and right cerebral hemispheres. All fibers were extracted from the mean DTI in standard space and are colored according to the SSC map. 3-dimensional white matter pathway reconstructions are presented above pathway termination coordinates in standard space. All termination coordinates are illustrated on a surface rendered FA map (FA $\geq$ 0.08) and colored according to the SSC map to enable assessment of the regions connected together by the tractography results. White matter pathways are annotated on the 3-dimensional streamline reconstructions, and anatomical regions (including BAs in parentheses) are annotated on the streamline termination maps. Gray matter: Ga, angular gyrus; Gsc, subcentral gyrus; GSm, supramarginal gyrus; GTi, inferior temporal gyrus; GTm, middle temporal gyrus; GTs, superior temporal gyrus; LPs, superior parietal lobule; MITi, middle-inferior temporal isthmus. White matter: AF, arcuate fasciculus; SPL, superior parietal lobule pathway.

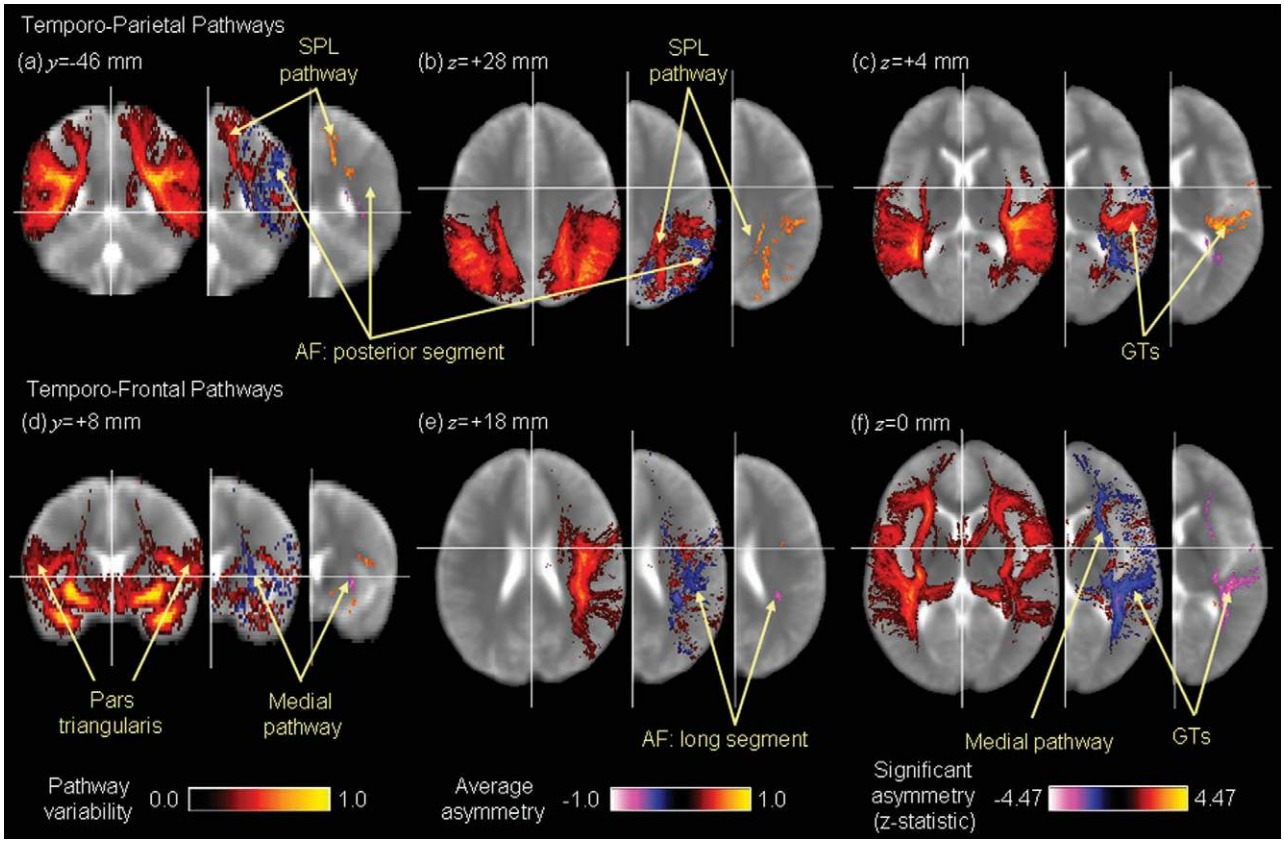

Figure 2. Pathway variability, asymmetry, and statistical significance maps of white matter pathways that pass between the temporal and parietal lobes (upper row) and the temporal and frontal lobes (lower row) are shown in neurological format for the 30 right-handed young healthy subjects overlain on the mean echo planar T_2-weighted image without diffusion sensitization. Intersubject pathway variability maps are illustrated using a hot color map (black = 0, to yellow = 1) and are presented for the left and right hemispheres in the same image slices. Asymmetry maps are shown adjacent to intersubject pathway variability maps in the right hemisphere only (as they are symmetrical about the midsagittal plane in standard space). These are colored using cold and hot colors to represent leftward (white = –1, to black = 0) and rightward asymmetry (yellow = 1, to black = 0), respectively. In particular, absolute values close to 1 represent pathway asymmetries that are present in all subjects, whereas absolute values close to 0 represent symmetry throughout the subjects. Finally, to the right of the asymmetry maps are significant asymmetry maps of the *z* statistic. Cold and hot colors represent significant leftward and rightward asymmetries, respectively. Gray matter: GTs, superior temporal gyrus. White matter: AF, arcuate fasciculus; SPL, superior parietal lobule pathway.

(black through blue and purple to white) colors, respectively. Significant asymmetry maps of the *z* statistic are shown to the right of the asymmetry maps in Figure 2. These significance maps are colored using the same color map used to represent the asymmetry maps.

The first pathway (highlighted by yellow arrows in Fig. 1), connecting the superior temporal lobe to the superior parietal lobule was clearly present in the right hemisphere as shown in Figure 1 with the pathway shown to exist in both hemispheres as indicated by the pathway variability maps in Figure 2. This pathway, referred to here as the superior parietal lobule pathway, has not been reported in previous tractography studies. The superior parietal lobule pathway began along the length of the superior temporal gyrus and the posterior end of the middle temporal gyrus. It passed medially for approximately 20 mm before sweeping superiorly and posteriorly into the superior parietal lobule. The anterior fibers terminated medially and superiorly, whereas the posterior fibers ended laterally and inferiorly. The superior parietal lobule pathway exhibited a large significant rightward asymmetry at its superior (Fig. 2*a*,*b*) and inferior limits (Fig. 2*c*).

The second pathway (highlighted by green arrows in Fig. 1) connected the superior, middle, and inferior temporal gyri (BA 21, 22, and 37) bilaterally to the inferior parietal lobule (Fig. 1). In more detail, the pathway began in the posterior, middle, and inferior temporal gyri (BA 21, 22, and 37) and passed medially (with a slight superior inclination) for a distance of approximately 15 mm before turning vertically upward into the inferior parietal lobule and merging with several fibers beginning exclusively in the superior temporal gyrus (BA 22). Here the pathway turned laterally into the supramarginal (BA 40) and angular gyri (BA 39). This pathway, recently referred to as the posterior segment of the arcuate fasciculus by Catani and others (2005), was found to have a significant leftward asymmetry (Fig. 2*a*,*b*).

Temporofrontal Pathway Morphology and Asymmetry

Two separate leftwardly asymmetric pathways between the posterior temporal lobe and the inferior frontal gyrus are shown in Figure 3. The first pathway (highlighted by blue arrows in Fig. 3) connected the posterior temporal lobe (BA 21, 22, and 37) to the precentral gyrus (BA 4 and 6) and pars opercularis (BA 44) via a dorsal route through the inferior parietal lobule. In more detail, the pathway began in the posterior, middle, and inferior temporal gyri (BA 21 and 37) and passed medially for approximately 15 mm before sweeping superiorly into the parietal lobe and merging with several fibers beginning in the superior temporal gyrus (BA 22). On reaching the parietal lobe, it passed anteriorly into the frontal lobe as far as the precentral gyrus

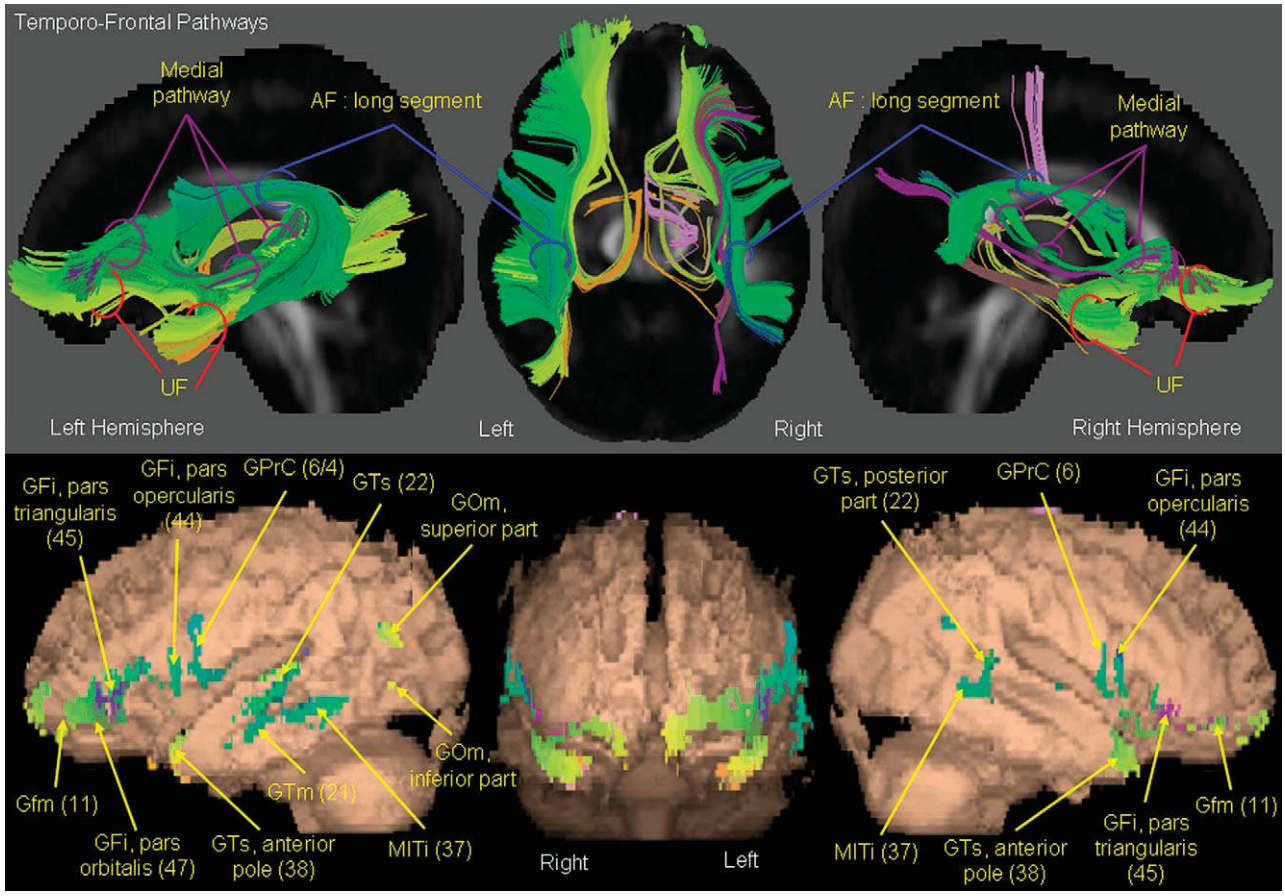

Figure 3. Temporofrontal white matter pathways. White matter fibers are illustrated that pass between the temporal and frontal lobes in the left and right cerebral hemispheres. All fibers were extracted from the mean DTI in standard space and are colored according to the SSC map. 3-dimensional white matter pathway reconstructions are presented above pathway termination coordinates in standard space. All termination coordinates are illustrated on a surface rendered FA map (FA $\geq$ 0.08) and colored according to the SSC map to enable assessment of the regions connected together by the tractography results. White matter pathways are annotated on the 3-dimensional streamline reconstructions, and anatomical regions (including BAs in parentheses) are annotated on the streamline termination maps. Gray matter: GFi, inferior frontal gyrus; Gfm, frontomarginal gyrus; GOm, middle occipital gyrus; GPrC, precentral gyrus; GTm, middle temporal gyrus; GTs, superior temporal gyrus; MITi, middle-inferior temporal isthmus. White matter: AF, arcuate fasciculus; UF, uncinate fasciculus.

(BA 4 and 6) where most fibers turned sharply toward the lateral surface. The remaining fibers continued to the pars opercularis of the inferior frontal gyrus (BA 44). This pathway, recently referred to as the long segment of the arcuate fasciculus by Catani and others (2005), was found to have a significant leftward asymmetry anteriorly in the long segment of the arcuate fasciculus (Fig. 2*d*), at the superior extent of the pathway (Fig. 2*e*), and in the posterior part of the superior and middle temporal gyri (Fig. 2*f*).

The second was a medial pathway (highlighted by purple arrows in Fig. 3) connecting the posterior temporal lobe (BA 21, 22, and 37) to the inferior frontal gyrus (BA 45 and 47). The pathway separated from the long segment of the arcuate fasciculus on reaching the parietal lobe and swept inferiorly and anteriorly through the external capsule to the anterior inferior frontal gyrus before fanning out into the pars triangularis (BA 45) and pars orbitalis (BA 47). Significant leftward asymmetry was revealed in the medial pathway, particularly in the external capsule (Fig. 2*d*,*f*).

Discussion

We have investigated the morphology and asymmetry of temporoparietal and temporofrontal white matter pathways by application of diffusion tensor tractography techniques to a data set of 30 right-handed young healthy subjects. Using novel visualization techniques, 4 asymmetrical white matter pathways were found to pass between the posterior temporal lobe and the parietal and frontal lobes. The main finding of the present study is a significant rightwardly asymmetric temporoparietal pathway connecting the superior temporal gyrus to the superior parietal lobule. Other findings include a significant leftwardly asymmetric temporoparietal pathway found connecting the posterior temporal lobe through the posterior segment of the arcuate fasciculus to the supramarginal and angular gyri. In addition, 2 significant leftwardly asymmetric temporofrontal pathways were found connecting the posterior temporal lobe to the frontal lobes. The first passed along the long (dorsal) segment of the arcuate fasciculus to the precentral gyrus and pars opercularis, whereas the second was a medial pathway through the external capsule to the pars triangularis and pars opercularis. Each of the above-mentioned pathways connected the middle and inferior temporal gyri as well as the superior temporal gyrus to the parietal and frontal lobes. In the following, these 4 pathways are discussed in the context of recent studies on the anatomy of auditory and language functions.

Our finding of a large rightward asymmetry in white matter pathways connecting the superior and middle temporal gyri to the superior parietal lobule has not been previously reported to our knowledge. Culham and Kanwisher (2001) report the human parietal lobe to be a functionally heterogeneous region, subserving a wide range of functions related to attention. In particular, the superior parietal lobule is a cortical region that integrates multimodal sensory information and provides guidance to motor operations through connections with the premotor cortex (Friedman and Goldman-Rakic 1994; Bushara and others 1999). Functional imaging studies have shown that the superior parietal lobule is part of a larger network involved in working memory of verbal (Gurd and others 2002; Crottaz-Herbette and others 2004), auditory spatial (Zatorre and others 1999; Arnott and others 2005), and auditory pitch tasks (Zatorre and others 1999; Gaab and others 2003). Several studies report lateralized right hemisphere processing of auditory spatial information in the superior parietal lobule (Griffiths and others 1998, 2000). The superior parietal lobule pathway has been implicated in combined aspects of auditory visual processing such as temporal and spatial aspects of audiovisual speech that have been shown to activate the superior temporal sulcus and an internal region of the right parietal lobe when auditory and visual sources are presented in opposite hemifields (Macaluso and others 2004).

Connections between the middle and superior temporal gyri and the supramarginal (BA 40) and angular (BA 39) gyri through the posterior segment of the arcuate fasciculus exhibited leftward asymmetry. This is consistent with tractography results reported by Parker and others (2005). As suggested by Catani and others (2005), this pathway may be involved in ideational speech; however, it is unlikely that these pathways are solely implicated in language processing. The angular gyrus and, in particular, the supramarginal gyrus have been shown to represent part of a larger network involved in auditory spatial and attentional functions (e.g., Griffiths and others 1998, 2000; Bushara and others 1999; Weeks and others 1999; Zatorre and others 1999, 2002; Alain and others 2001; Maeder and others 2001). This is further supported by a meta-analysis of the auditory dual-pathway (what–where) model (Arnott and others 2004). Arnott and others (2004) reported the bilateral activation of the supramarginal gyrus in 50% of studies. However, there are several studies supporting greater functional activity in the right inferior parietal lobule than the left for auditory spatial and attentional processing (Griffiths and others 1998; Weeks and others 1999; Zatorre and others 1999, 2002; Griffiths and others 2000; Itoh and others 2000; Alain and others 2001; Brunetti and others 2005). In the context of the leftward asymmetry of the posterior segment of the arcuate fasciculus, it seems that overall the leftward asymmetry in right-handed subjects is related to lateralization of language, rather than auditory spatial function.

Our finding of dorsal white matter pathway connections to the frontal lobe via the long segment of the arcuate fasciculus is consistent with tractography results obtained by Catani and others (2005) for the left cerebral hemisphere and Parker and others (2005) for both cerebral hemispheres. These results are consistent with a recently emerging functional model of language perception hypothesized from lesion, positron emission tomography, functional magnetic resonance imaging, electrocortical mapping by cortical stimulation, and hemispheric anesthesia by intracorotid amobarbitol studies (Boatman 2004; Hickok and Poeppel 2004; Scott and Wise 2004). In particular, Hickok and Poeppel suggest the existence of bilateral (but leftwardly asymmetrical) dorsal functional pathways between the superior temporal gyrus and a posterior inferior frontal region including various parts of Broca's area, the frontal operculae, the motor face area, and dorsal premotor cortex. These pathways (apart from those to the dorsal premotor cortex) are identified by our analysis and are shown to be leftwardly asymmetric. In addition, we found a leftwardly asymmetric medial pathway connecting the superior temporal gyrus through the external capsule to the pars triangularis and pars orbitalis. Parker and others (2005) also found this pathway but referred to it as ventral rather than medial. As to the potential functional processing of this pathway, the pathway connects the posterior temporal lobe to BA 46 and BA 47, and these regions have been recently implicated in verbal working memory functions (Cabeza and Nyberg 2000; Dronkers and others 2004).

Dorsal and medial temporofrontal pathways were found to have extensive connections with the middle and inferior temporal gyri, particularly in the left hemisphere. These regions primarily correspond with the location of the posterior and anterior sections of BA 21 and BA 37, respectively. It seems reasonable that white matter pathways should emanate from this region, particularly in the left hemisphere, as the middle temporal gyrus has been shown to be important in speech production (Indefrey and Levelt 2004). Furthermore, the middle temporal gyrus (posterior BA 21 and anterior BA 37) has been implicated in word-level processing and generation (Cabeza and Nyberg 2000; Dronkers and others 2004).

There are several limitations of the applied techniques that are now discussed. First, the Talairach Daemon was used to segment the temporal, parietal, and frontal lobes from the normalized DTI data. Necessarily, the Talairach Daemon segmentation will be imprecise at lobe boundaries due to inaccuracies accrued by image registration to standard space. However, such registration errors are limited to lobe boundaries, and because the white matter pathways of interest are not located exclusively at lobe boundaries, these errors will have little effect on our findings. Second, the applied tractography technique does not account for regions of white matter fiber crossing in the human brain. Recently, high angular resolution diffusion–imaging and associated analysis techniques, such as q-ball imaging (Tuch and others 2002), persistent angular structure MRI (Jansons and Alexander 2003), and spherical deconvolution (Tournier and others 2004), have been proposed to resolve this problem but have not yet been validated anatomically. In addition, application of tractography methods to crossing data is not straightforward due to noise propagation into the diffusion profiles and the detection of false-positive crossings. However, white matter pathways of the brain have been faithfully reconstructed using diffusion tensor tractography without invoking methodology to resolve fiber crossing (e.g., Catani and others 2002, 2003, 2005). Furthermore, the pathways of interest segmented in the present study do not pass through fiber-crossing regions reported in previous tractography studies.

In conclusion, we have applied a new fully automated lobe-based tractography technique to investigate the underlying morphology and asymmetry of white matter pathways associated with the posterior temporal lobe and its connections to the parietal and frontal lobes. For the first time, a significant rightwardly asymmetric pathway connecting the temporal lobe to the superior parietal lobule was identified. This pathway may be

related to auditory spatial attention and working memory for which there is evidence for a rightward lateralization from functional imaging studies. Additional significant leftward asymmetries connecting the parietal and frontal lobes to the temporal lobe may be more closely related to laterality of language. This study highlights the potential of DTI and tractography techniques to discern white matter pathways of functional relevance in the human brain in vivo, indicating a close association between asymmetric white matter organization and lateralized brain function.

Notes

This research was funded by Research into Aging fellowship #259. All 3-dimensional white matter pathway reconstructions were displayed using Geomview, http://www.geomview.org. All medical image slices and white matter surface renderings were displayed using mri3dX, http://www-users.aston.ac.uk/~singhkd/mri3dX/. Thanks also to Rebecca Charlton and Arani Nitkunan for their assistance in MRI data acquisition. *Conflict of Interest*: None declared.

Address correspondence to Dr Thomas Barrick, Centre for Clinical Neuroscience, Division of Cardiac and Vascular Sciences, St George's University of London, Cranmer Terrace, London SW17 0RE, UK. Email: tbarrick@sgul.ac.uk.

References

Alain C, Arnott SR, Hevenor S, Graham S, Grady CL. 2001. "What" and "where" in the human auditory system. Proc Natl Acad Sci USA 98(21):12301–12306.

Arnott SR, Binns MA, Grady CL, Alain C. 2004. Assessing the auditory dual pathway model in humans. Neuroimage 22:401–408.

Arnott SR, Grady CL, Hevenor SJ, Graham S, Alain C. 2005. The functional organization of auditory working memory as revealed by fMRI. J Cogn Neurosci 17(5):819–831.

Barrick TR, Clark CA. 2004. Singularities in diffusion tensor fields and their relevance in white matter fiber tractography. Neuroimage 22(2):481–491.

Barrick TR, Lawes INC, Clark CA. 2004. White matter pathway asymmetry corresponds to auditory-spatial and language lateralisation. Proceedings of the 12th Meeting of the International Society for Magnetic Resonance in Medicine; Kyoto, Japan; 2004 May 15–16. 314 p.

Barrick TR, Mackay CE, Prima S, Maes F, Vandermeulen D, Crow TJ, Roberts N. 2005. Automatic analysis of cerebral asymmetry: an exploratory study of the relationship between brain torque and planum temporale asymmetry. Neuroimage 24:678–691.

Basser PJ, Mattiello J, LeBihan D. 1994. Estimation of the effective self-diffusion tensor from the NMR spin echo. J Magn Reson B 103:247–254.

Behrens TE, Johansen-Berg H, Woolrich MW, Smith SM, Wheeler-Kingshott CA, Boulby PA, Barker GJ, Sillery EL, Sheehen K, Ciccarelli O, Thompson AJ, Brady JM, Matthews PE. 2003. Non-invasive mapping of connections between human thalamus and cortex using diffusion imaging. Nat Neurosci 6(7):750–757.

Boatman D. 2004. Cortical bases of speech perception: evidence from functional lesion studies. Cognition 92(1–2):47–65.

Broca P. 1861. Remarques sur la siegé de la faculté du langue. Bull Soc Anat Paris 6:330–357.

Brunetti M, Belardinelli P, Caulo M, Del Gratta C, Della Penna S, Ferretti A, Lucci G, Moretti A, Pizella V, Tartaro A, Torquati K, Olivetti Belardinelli M, Romani GL. 2005. Human brain activation during passive listening to sounds from different location: an fMRI and MEG study. Hum Brain Mapp 26(4):251–261.

Bushara KO, Weeks RA, Ishii K, Catalan MJ, Tian B, Rauscheeker JP, Hallett M. 1999. Modality-specific frontal and parietal areas for auditory and visual spatial localization in humans. Nat Neurosci 2(8):759–766.

Cabeza R, Nyberg L. 2000. Imaging cognition II: an empirical review of 275 PET and fMRI studies. J Cogn Neurosci 12(1):1–47.

Catani M, Howard RJ, Pajevic S, Jones DK. 2002. Virtual in vivo dissection of white matter fasiculi in the human brain. Neuroimage 17(1):77–94.

Catani M, Jones DK, Donato R, Ffytche DH. 2003. Occipito-temporal connections in the human brain. Brain 126(9):2093–2107.

Catani M, Jones DK, Ffytche DH. 2005. Perisylvian language networks of the human brain. Ann Neurol 57:8–16.

Clarke S, Bellmann A, Meuli RA, Assal G, Steck AJ. 2000. Auditory agnosia and auditory spatial deficits following left hemispheric lesions: evidence for distinct processing pathways. Neuropsychologia 38:797–807.

Clarke S, Thiran Bellmann A, Maeder P, Adriana M, Vernet O, Regli L, Cuisenaire O, Thiran J.-P. 2003. What and where in human audition: selective deficits following focal hemispheric lesions. Exp Brain Res 147:8–15.

Crottaz-Herbette S, Anagnoson RT, Menon V. 2004. Modality effects in verbal working memory: differential prefrontal and parietal responses in auditory and visual stimuli. Neuroimage 21:340–351.

Culham JC, Kanwisher NG. 2001. Neuroimaging of cognitive functions in human parietal cortex. Curr Opin Neurobiol 11(2):157–163.

Davidson RJ, Hugdahl K, editors. 1995. Brain asymmetry. Cambridge, MA: MIT Press.

Dronkers NF, Wilkins DP, Van Valin RD Jr, Redfern BB, Jaeger JJ. 2004. Lesion analysis of the brain areas involved in language comprehension. Cognition 92(1–2):145–177.

Evans AC, Collins DL, Mills SR, Brown ED, Kelly RL, Peters TM. 1993. 3D statistical neuroanatomical models from 305 MRI volumes. Proceedings of IEEE-Nuclear Science Symposium and Medical Imaging Conference; Piscataway, New York: IEEE press. p 1813–1817.

Friedman HR, Goldman-Rakic PS. 1994. Coactivation of prefrontal cortex and inferior parietal cortex in working memory tasks revealed by 2DG functional mapping in the rhesus monkey. J Neurosci 14(5):2775–2788.

Gaab N, Gaser C, Zaehle T, Jancke L, Schlaug G. 2003. Functional anatomy of pitch memory—an fMRI study with sparse sampling. Neuroimage 19:1417–1426.

Geschwind N, Levitsky W. 1968. Human brain left-right asymmetries in temporal speech region. Science 161:186–187.

Geschwind N, Levitsky W. 1991. Left-right asymmetry in temporal speech region. Biol Psychiatry 29:159–175.

Good CD, Johnsrude I, Ashburner J, Henson RNA, Friston KJ, Frackowiak RSJ. 2001. Cerebral asymmetry and the effects of sex and handedness on brain structure: a voxel-based morphometric analysis of 465 normal adult human brains. Neuroimage 14:685–700.

Griffiths TD, Green GGR, Rees A, Rees G. 2000. Human brain areas involved in the analysis of movement. Hum Brain Mapp 9:72–80.

Griffiths TD, Rees G, Rees A, Green GGR, Witton C, Rowe D, Buchel C, Turner R, Frackowiak RSJ. 1998. Right parietal cortex is involved in the perception of sound movement in humans. Nature 1(1):74–79.

Griffiths TD, Warren JD. 2002. The planum temporale as a computational hub. Trends Neurosci 25(7):348–353.

Gurd JM, Amunts K, Weiss PH, Zafiris O, Zilles K, Marshall JC, Fink GR. 2002. Posterior parietal cortex is implicated in continuous switching between verbal fluency tasks: an fMRI study with clinical implications. Brain 125:1024–1038.

Hagmann P, Thiran JP, Jonasson L, Vandergheynst P, Clarke S, Maeder P, Meuli R. 2003. DTI mapping of human brain connectivity: statistical fibre tracking and virtual dissection. Neuroimage 19(3):545–554.

Hickok G, Poeppel D. 2004. Dorsal and ventral streams: a framework for understanding aspects of the functional anatomy of language. Cognition 92(1–2):67–99.

Indefrey P, Levelt WJ. 2004. The spatial and temporal signatures of word production components. Cognition 92(1–2):101–144.

Itoh K, Yumoto M, Uno A, Kurauchi T, Kaga K. 2000. Temporal stream of cortical representation for auditory spatial localization in human hemispheres. Neurosci Lett 292:215–219.

Jansons KM, Alexander DC. 2003. Persistent angular structure: new insights from diffusion magnetic resonance imaging data. Inverse Probl 19:1031–1046.

Johansen-Berg H, Behrens TE, Sillery E, Ciccarelli O, Thompson AJ, Smith SM, Matthews PM. 2005. Functional-anatomical validation and in-

dividual variation of diffusion tractography-based segmentation of the human thalamus. Cereb Cortex 15(1):31–39.
Jones DK, Griffin LD, Alexander AC, Catani M, Horsfield MA, Howard R, Williams SCR. 2002. Spatial normalization and averaging of diffusion tensor MRI datasets. Neuroimage 17:592–617.
Lancaster JL, Woldorff MG, Parsons LM, Liotti M, Freitas CS, Rainey L, Kochunov PV, Nickerson D, Mikiten SA, Fox PT. 2000. Automated Talairach atlas labels for functional brain mapping. Hum Brain Mapp 10:120–131.
Macaluso E, George N, Dolan R, Spence C, Driver J. 2004. Spatial and temporal factors during processing of audio-visual speech: a PET study. Neuroimage 21:725–732.
Maeder PP, Meuli R, Adriani M, Bellmann A, Fornari E, Thiran J-P, Pittet A, Clarke S. 2001. Distinct pathways involved in sound recognition and localisation: a human fMRI study. Neuroimage 14:802–816.
Mori S, Kaufmann WE, Davatzikos C, Stieltjes B, Amodei L, Fredericksen K, Pearlson GlD, Melhem ER, Solaiyappan M, Raymond GV, Moser HW, van Zijl PCM. 2002. Imaging cortical association tracts in the human brain using diffusion-tensor-based axonal tracking. Magn Reson Med 47:215–223.
Parker GJM, Luzzi S, Alexander DC, Wheeler-Kingshott CAM, Ciccarelli O, Ralph MAL. 2005. Lateralisation of ventral and dorsal auditory-language pathways in the human brain. Neuroimage 24:656–666.
Pierpaoli C, Basser PJ. 1996. Toward quantitative assessment of diffusion anisotropy. Magn Reson Med 36:893–906.
Rauscheker JP. 1998. Parallel processing in the auditory cortex of primates. Audiol Neurootol 3:86–103.
Romanski LM, Tian B, Fritz J, Mishkin M, Goldman-Rakic PS, Rauscheker JP. 1999. Dual streams of auditory afferents target multiple domains in the primate prefrontal cortex. Nat Neurosci 2(12):1131–1136.
Rumsey JM, Dorwast R, Verness M, Denkla MB, Kruesi JP, Rapport JL. 1986. Magnetic resonance imaging of the brain anatomy in severe developmental dyslexia. Arch Neurol 43:1045–1046.
Scott SK, Wise RJS. 2004. The functional neuroanatomy of prelexical processing in speech perception. Cognition 92(1–2):13–45.
Shapleske J, Rossell SL, Woodruff PW, David AS. 1999. The planum temporale: a systematic, quantitative review of its structural, functional and clinical significance. Brain Res Rev 29(1):26–49.
Siegel S. 1956. Nonparametric statistics for the behavioral sciences. New York: McGraw-Hill.
Smith SM. 2002. Fast robust automated brain extraction. Hum Brain Mapp 17(3):143–155.
Stieltjes B, Kaufmann WE, van Zijl PCM, Fredericksen K, Pearlson GD, Solaiyappan M, Mori S. 2001. Diffusion tensor imaging and axonal tracking in the human brainstem. Neuroimage 14(3):723–735.
Tournier JD, Calamante F, Gadian DG, Connelly A. 2004. Direct estimation of the fiber orientation density function from diffusion-weighted MRI data using spherical deconvolution. Neuroimage 23(3):1176–1185.
Tuch DS, Reese TG, Wiegell MR, Makris N, Belliveau JW, Wedeen VJ. 2002. High angular resolution diffusion imaging reveals intravoxel white matter fiber heterogeneity. Magn Reson Med 48(4): 577–582.
Watkins KE, Paus T, Lerch JP, Zijdenbos A, Collins DL, Neelin P, Taylor J, Worsley KJ, Evans AC. 2001. Structural asymmetries in the human brain: a voxel-based statistical analysis of 142 MRI scans. Cereb Cortex 11:868–877.
Weeks RA, Aziz-Sultan A, Bushara KO, Tian B, Wessiger CM, Dang N, Rauscheker JP, Hallett M. 1999. A PET study of human auditory spatial processing. Neurosci Lett 262:155–159.
Woods RP, Maziotta JC, Cherry SR. 1993. MRI-PET registration with automated algorithm. J Comput Assisted Tomogr 17(4): 536–546.
Zatorre RJ, Bouffard M, Ahad P, Belin P. 2002. Where is 'where' in the human auditory cortex? Nat Neurosci 5(9):905–909.
Zatorre RJ, Mondor TA, Evans AC. 1999. Auditory attention to space and frequency activates similar cerebral systems. Neuroimage 10: 544–554.